

RSC Advances



This is an *Accepted Manuscript*, which has been through the Royal Society of Chemistry peer review process and has been accepted for publication.

Accepted Manuscripts are published online shortly after acceptance, before technical editing, formatting and proof reading. Using this free service, authors can make their results available to the community, in citable form, before we publish the edited article. This *Accepted Manuscript* will be replaced by the edited, formatted and paginated article as soon as this is available.

You can find more information about *Accepted Manuscripts* in the [Information for Authors](#).

Please note that technical editing may introduce minor changes to the text and/or graphics, which may alter content. The journal's standard [Terms & Conditions](#) and the [Ethical guidelines](#) still apply. In no event shall the Royal Society of Chemistry be held responsible for any errors or omissions in this *Accepted Manuscript* or any consequences arising from the use of any information it contains.

Cite this: DOI: 10.1039/c0xx00000x

www.rsc.org/xxxxxx

COMMUNICATIONS

A TTFV–pyrene-based copolymer: synthesis, redox properties, and aggregation behaviour

Eyad A. Younes, Kerry-Lynn M. Williams, Joshua C. Walsh, Celine M. Schneider, Graham J. Bodwell* and Yuming Zhao*

Received (in XXX, XXX) XthXXXXXXXXXX 20XX, Accepted Xth XXXXXXXXXXXX 20XX
DOI: 10.1039/b000000x

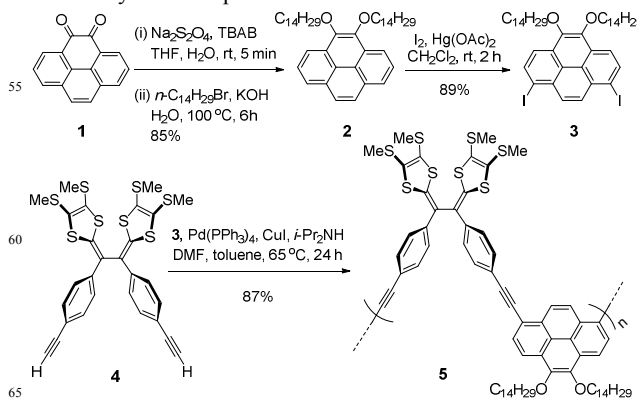
A new π -conjugated copolymer containing tetrathiafulvalene vinylogue (TTFV) and pyrene repeat units was synthesized and found to exhibit reversible redox activity, while the self-aggregation behaviour in solution phase was found to be responsive to external stimuli such as the nature of the solvent and the pH value.

π -Conjugated polymers bearing redox active units have found widespread applications in organic semiconducting materials and optoelectronic devices.¹ Synthetically, incorporation of the redox active components (e.g. electron donors or acceptors) can be attained by having them either embedded in the polymer backbone or appended to the side chains.^{1b,c} Tetrathiafulvalene vinylogues (TTFVs) have received growing attention over the past few years in the design of novel redox-active molecules and polymers, owing to their excellent electron-donating properties.² Of particular interest is the class of aryl-substituted TTFVs, which show not only rich electrochemical activity, but also intriguing conformational switching behaviour associated with redox reactions.^{2a,3} We and others have recently demonstrated that the incorporation of TTFVs in various π -conjugated systems can afford useful functional molecular materials and devices, ranging from redox-switchable ligands,⁴ stimuli-responsive foldamers⁵ and shape-persistent macrocycles⁶ to redox-regulated molecular rotors,⁷ synthetic receptors and chemosensors.⁸

In the design of aryl-based π -conjugated materials, pyrene is often chosen as a favourable π -building block because of its remarkable photophysical properties as well as its redox activity.⁹ Furthermore, pyrene tends to interact strongly with other aromatic systems via π -stacking, which can be utilized to generate pre-organized supramolecular assemblies.¹⁰ The combination of TTFV and pyrene has been demonstrated to be an appealing design approach to attain novel supramolecular properties. For example, we previously developed a class of pyrene–TTFV-based molecular tweezers that exhibit selective binding to C₇₀ fullerene in the presence of a large excess of C₆₀.^{8c} Along the same lines, we further envisioned that copolymers made of TTFV and pyrene moieties should give rise to very interesting redox activity and supramolecular behaviour that might be useful in materials applications.

For the most part, pyrenylene units that have been placed in π -extended structures have had either 1,6-, 1,8- or 2,7-substitution patterns.¹¹ The 1,8-substitution pattern has been exploited in our

recent research, which has led to the synthesis of some shape-persistent macrocycles.¹² Copolymer systems that incorporate both TTFV and pyrenylene systems as repeat units, however, have not yet been reported in the literature.



Scheme 1. Synthesis of TTFV–pyrene-based copolymer 5 via Sonogashira coupling polymerization.

In this work, we report the synthesis and characterization of the first TTFV–pyrene-based copolymer 5. Acetylenic TTFV 4 and 1,8-diiodo-4,5-bis(tetradecyloxy)pyrene 3 were identified as two key building blocks for the synthesis of 5. The 1,8-pyrenylene pattern was chosen to impart a repeating bend (120°) in the polymer backbone, which was expected to provide access to folded/helical structures. OC₁₄H₂₉ side chains were chosen to promote solubility of the copolymer 5. Diyne 4 was synthesized according to literature procedures,⁶ whereas diiodide 3 was synthesized in short order from diketone 1¹² (Scheme 1). One-pot reductive alkylation of 1 afforded 4,5-dialkoxyppyrene 2 (85%), which was iodinated under mild conditions to afford diiodide 3 (88%) with complete 1,8-regioselectivity. The copolymerization of 3 and 4 was conducted under Sonogashira conditions (Pd(PPh₃)₄/CuI, *i*-Pr₂NH) in DMF/toluene at 65 °C. The resulting crude polymer was purified by precipitation from MeOH, followed by exhaustive rinsing with MeOH, giving 5 as a yellow solid in 87% yield. Copolymer 5 was found to be non-fluorescent in both solution and the solid state, due to the strong quenching effect of the electron-donating TTFV moiety.

TTFV–pyrene-based copolymer 5 was characterized by ¹H NMR and IR spectroscopy (see ESI). According to GPC analysis, *M*_w=6,219 g mol⁻¹, *M*_n=4,562 g mol⁻¹ and PDI=1.32. The GPC

data suggest that the average chain length of copolymer **5** is at the stage of the pentamer. The conformational properties of **5** were then studied through molecular mechanics (*MM*) simulations. Using the *MMFF* force field implemented in the Spartan'10 software,¹³ conformations at two extremities were optimized (Figure 1). The first conformer takes a zig-zag structure (Figure 1A), where the TTFV and pyrene moieties do not have any intramolecular π -stacking. The second one is a foldamer (Figure 1B and 1C), in which the TTFV and pyrene units are tightly packed together through π - π interactions, such that the folded structure takes a cylinder-like shape. The central cavity of the foldamer is calculated to be too small (*ca.* 0.4-0.5 nm) to encapsulate meaningful organic guest molecules. Calculations show that the foldamer is roughly 31.0 kcal mol⁻¹ more stable than the zig-zag conformer (in the gas phase), suggesting the polymer has a strong preference for assuming the folded conformation as a result of self-aggregation. Pulsed gradient spin-echo (PGSE) NMR analysis shows that copolymer **5** has an average diffusion coefficient (*D*) of 1.984×10^{-10} m² s⁻¹, which corresponds to a hydrodynamic radius of 2.13 nm according to the Stokes-Einstein equation (see the ESI for details). Considering that the computational work on **5** used OCH₃ groups and H atoms instead of OC₁₄H₂₉ and SCH₃ groups respectively, the diffusion NMR data agrees reasonably well with the calculated molecular dimensions of the folded conformer (see Figure 1B and 1C) and hence suggests that the folded conformation of **5** is highly favoured in solution.

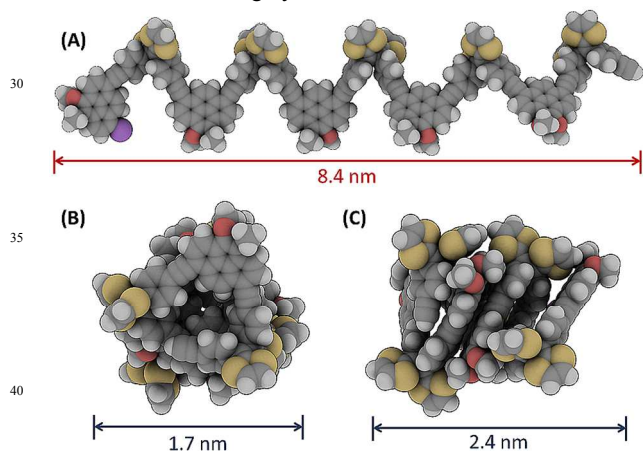


Figure 1. (A) Copolymer **5** in a zig-zag conformation. (B) Front view, and (C) side view of **5** in a fully folded conformation. The geometries were optimized using the *MMFF* force field. To save computational cost, the OC₁₄H₂₉ and SCH₃ groups in **5** were replaced by OCH₃ groups and H atoms, respectively.

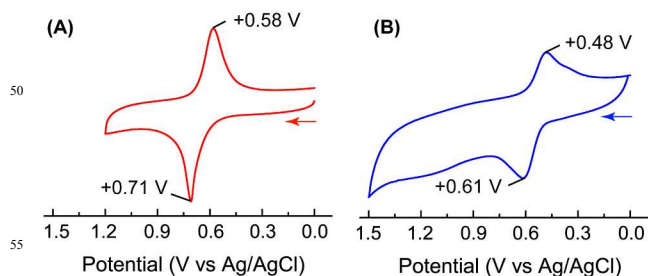


Figure 2. Cyclic voltammograms of (A) the thin film of copolymer **5** and (B) acetylenic TTFV **4**. Experimental conditions: solvent: CH₃CN; electrolyte: Bu₄NBF₄ (0.1 M); working electrode: glassy carbon; counter

electrode: Pt wire; reference electrode: Ag/AgCl (3 M NaCl); scan rate: 0.1 V s⁻¹.

The electrochemical redox properties of TTFV-pyrene copolymer **5** were investigated by cyclic voltammetry (CV). The CV profile measured for a thin film of **5** cast on the surface of a glassy carbon working electrode exhibits a reversible redox wave pair ($E_{pa} = +0.71$ V, $E_{pc} = +0.58$ V) with a formal potential ($E^{0'}$) at +0.64 V (Figure 2A). This redox pair can be assigned to the simultaneous two-electron transfer at the TTFV unit during the redox processes.^{2,3} In comparison to the redox behaviour observed for TTFV precursor **4**, the cathodic and anodic peaks of copolymer **5** are both shifted to the positive direction by +0.10 V. Such a significant anodic shift is similar to the CV behaviour of a TTFV-based shape-persistent macrocycle we previously studied, in which the TTFV unit was constrained to a pseudo *s-cis* conformation.⁶ Since the folded conformation of **5** bears more resemblance to the structure of the constrained rigid macrocycle than the unfolded one, this may be taken as an indication that the dominant conformation of copolymer **5** in the solid state is also the self-aggregated foldamer.

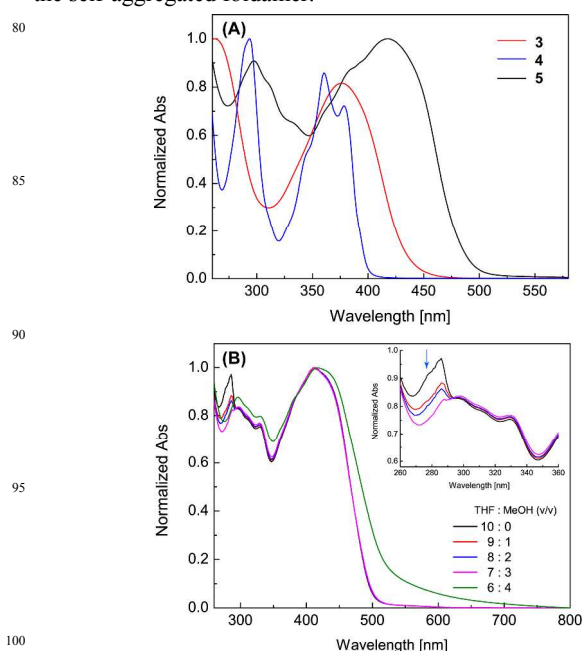


Figure 3. (A) UV-Vis absorption spectra of compounds **3-5** measured in CHCl₃ at room temperature. (B) UV-Vis spectra of copolymer **5** in THF/MeOH. Inset: expanded spectra (260-360 nm) showing copolymer **5** in THF/MeOH at volumetric ratios from 10:0 to 6:4.

The electronic absorption properties of copolymer **5** and its two precursors **3** and **4** were examined by UV-Vis spectroscopy (Figure 3A). In chloroform, copolymer **5** exhibits two absorption bands at 417 and 298 nm. Additionally, a number of shoulder bands are discernible at 383, 361, 333, and 312 nm. The spectrum of TTFV precursor **4** shows two absorption bands at 376 and 261 nm, while the spectrum of pyrene **3** gives characteristic vibronic progression at 379, 360, 344 (sh) nm, along with a high-energy band at 293 nm. Compared with the spectra of **3** and **4**, the lowest-energy absorption band of copolymer **5** is substantially red-shifted, presumably due to its extended π -delocalization.

Protic dipolar solvents (*e.g.* water, MeOH) are known to enhance folding and aggregation of arene-based conjugated

polymers, leading to significant changes in UV-Vis absorption.¹⁴ To investigate the solvent-dependent UV-Vis absorption properties of **5**, MeOH was gradually added to a THF solution of **5** and the process was monitored by UV-Vis analysis. As can be seen in Figure 3B, the stepwise increase in the proportion of MeOH in the polymer solution causes a two-stage change in the UV-Vis spectra. In the first stage, when the percentage of MeOH is increased from 0% to 30% (v/v), only the absorption band at 286 nm is observed to decrease in intensity, while the other regions of the spectrum do not show any significant variations. In the second stage (*i.e.* when the percentage of MeOH is increased beyond 30%), the spectrum undergoes more substantial changes: the lowest energy absorption maximum is redshifted and a pronounced low-energy absorption tail emerges.

The observed solvent-dependent UV-Vis absorption behaviour suggests that copolymer **5** may undergo dramatic changes in aggregation with increasing solvent polarity. To further understand the microscopic origins for these properties, MeOH (50 μ L per portion) was gradually added to a solution of copolymer **5** (3 mg) in THF (1 mL) to induce the formation of polymer aggregates. Dynamic light scattering (DLS) measurements were performed to determine the size range of the polymer aggregates (see Figure 4). When the volumetric ratio of THF:MeOH was gradually increased from 10:0 to 10:3, narrowly distributed particles with an average diameter of *ca.* 240 nm were detected in the solution. As the ratio of THF:MeOH was further increased to 10:6, the average diameter of the particles grew steadily to *ca.* 620 nm. Once the ratio reached 10:7, much larger particles (*ca.* 6.5 μ m in diameter) started to form and the size distribution was found to be very broad. In the meantime, the solution became visibly turbid, which is indicative of precipitation.

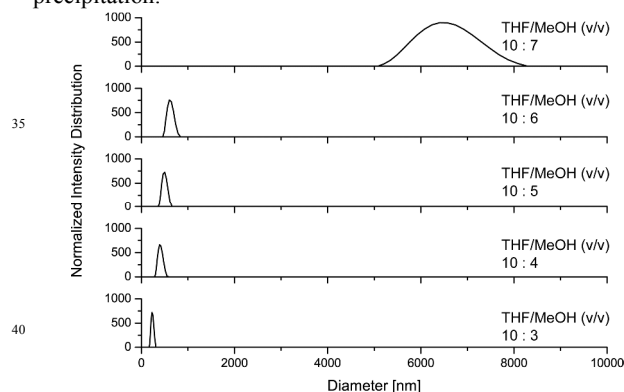


Figure 4. DLS analysis of the diameters of polymer aggregates formed in mixture solvent of THF/MeOH at various volumetric ratios.

The DLS results clearly indicate that the aggregation of copolymer **5** proceeds in two drastically different ways with increasing solvent polarity. Initially, aggregates are formed as relatively uniform nanoparticles, which can be correlated to the first-stage change observed in the solvent-dependent UV-Vis analysis (see inset of Figure 3b). Secondly, much larger micron-scale particles start to form, which is presumably responsible for the pronounced second-stage UV-Vis absorption changes in Figure 3B.

The kinetics of the MeOH-induced aggregation of **5** in THF appear to be complex and show significant dependence on factors

such as time, local concentration, and pH value. Figure 5 depicts the time-dependent size variation for the nanoparticles formed in 10:3 THF/MeOH. Within the first 45 min, the nanoparticles did not show any significant changes in size. After standing at room temperature for 75 min, the nanoparticles were found to decrease considerably in number, while more numerous and broadly distributed micron-sized particles began to form. Evidently, the narrowly distributed nanoparticles are metastable and tend to aggregate into much larger particles as a function of time.

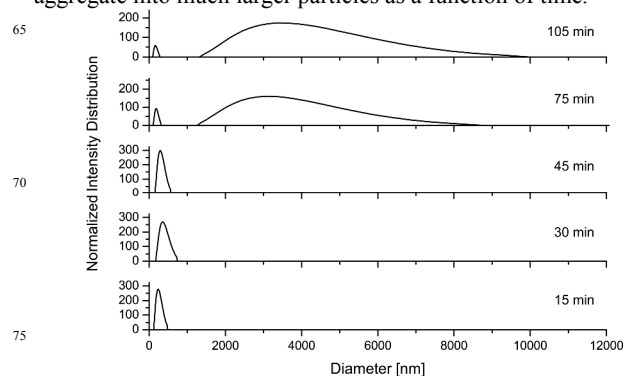


Figure 5. DLS analysis monitoring the diameter distribution of the aggregates of polymer **1** (3 mg) in THF/MeOH (10:3, v/v) at different periods of time at room temperature.

The way of adding MeOH to a THF solution of **5** was found to strongly affect the nature of the aggregation. When MeOH was added in one portion, instead of slow addition in small portions, to a THF solution of copolymer **5** to afford a 10:4 THF/MeOH ratio (v/v), a very broad size distribution was observed (see Figure 6). A plausible explanation is that the one-shot addition of MeOH resulted in instantaneously high local concentrations of MeOH in the solution, which in turn promoted the aggregation.

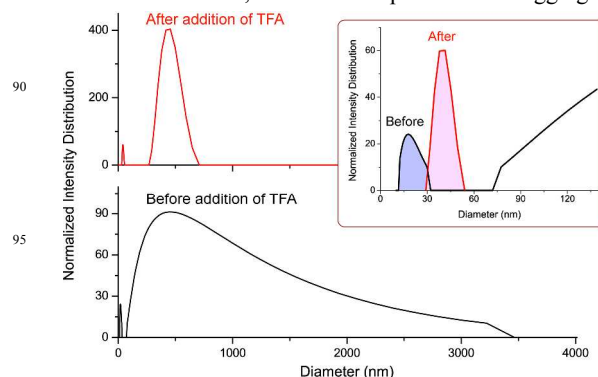


Figure 6. DLS analysis showing the diameter distribution of polymer aggregates in 10:4 THF/MeOH before and after addition of TFA. Inset: expansion of the size distributions in the region of 0 to 130 nm.

As the conformation of the TTFV moiety is known to be sensitive to pH,^{5b-c} the possibility of altering particle sizes via protonation of **5** with trifluoroacetic acid (TFA) was then tested. In this experiment, a tiny amount (*ca.* 1 μ L) of TFA was added to the THF/MeOH solution of **5** generated by one-portion MeOH addition. DLS analysis of the acidified mixture showed that the diameter distribution of the protonated aggregates was reversed to a much narrower profile as shown in Figure 6. It can also be noted that there was a small portion of particles with an average diameter of *ca.* 18 nm detected in the polymer solution (see the inset in Figure 6). These particles are likely due to micelles of

copolymer **5**. After addition of TFA, the average diameter of these micelles was observed to increase to *ca.* 40 nm. Protonation of TTFV by TFA has been known to considerably change the conformation of TTFV from a pseudo *s-cis* to a *s-trans* orientation.^{5b,c} Following this rationale, the entire framework of TTFV-pyrene copolymer **5** upon protonation is expected to change from the folded to a zig-zag like structure. Such a dramatic conformational change may account for the significantly increased micellar diameter after treatment with TFA.

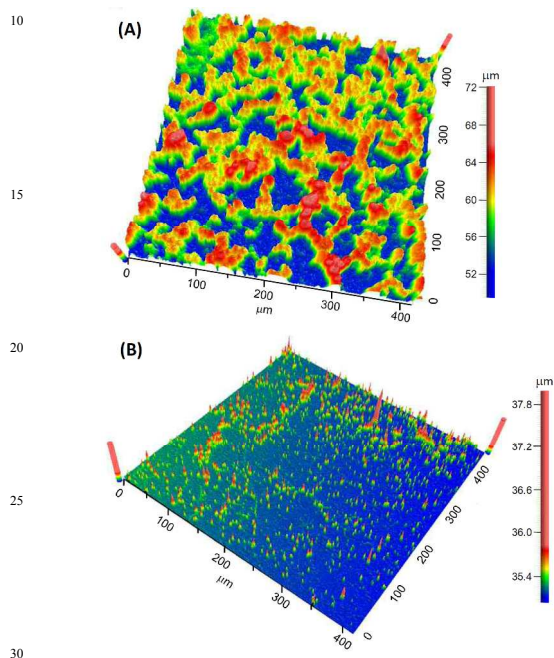


Figure 8. Surface topography for the thin film of copolymer **5** deposited on a glass substrate (A) before and (B) after exposure to TFA vapour for 20 min.

The responsiveness of the aggregates of copolymer **5** to TFA treatment at a surface was examined by optical surface profiling. As shown in Figure 8A, a solid film of **5** dropcast on the surface of a glass slide exhibits “worm-like” structures on the scale of tens of microns in height and hundreds of microns in length. These features indicate strong inter-polymer aggregation in the neutral solid state. After exposure to TFA vapour for *ca.* 20 min, the surface pattern was found to change substantially into a morphology featuring more dispersed and particle-like pattern, with considerably reduced discrete dimensions. The surface profiling results confirm that the aggregation of copolymer **5** in the solid state is also responsive to pH, and such a property can be utilized as a “bottom-up” control over the solid-state assembly and ordering at the microscopic level.

In conclusion, we have synthesized and investigated a new type of redox-active TTFV-pyrene-based copolymer **5**. The aggregation of the polymer evolves in two distinct stages (“nano” and “micron”) and shows dependence on solvent polarity, time, and pH. Even in the solid state, the polymer aggregates exhibit significant responsiveness to acidic vapours. We anticipate that this type of copolymer can be further developed to “intelligent” materials with controllable microscopic structures and programmable responsiveness to external stimuli (*e.g.* pH, solvent, and redox conditions).

Acknowledgements

We thank NSERC, CFI, and Memorial University for funding support. Prof. Alex Adronov of McMaster University is acknowledged for assistance in GPC analysis, and Prof. Qiying Chen of Memorial University is acknowledged for help in surface optical profiling analysis.

Notes and references

- ⁶⁵ Department of Chemistry, Memorial University, St. John's, NL, Canada A1B 3X7. Fax: 1 (709) 864-3702; Tel: 1 (709) 864-8747; E-mail: gbdowell@mun.ca; yuming@mun.ca.
- [†] Electronic Supplementary Information (ESI) available: Detailed synthetic procedures and analytical data for copolymer **5**. See DOI: 10.1039/b000000x/
- (a) G. Inzelt, *Conducting Polymers: A New Era in Electrochemistry*, Springer-Verlag, Berlin Heidelberg, 2008; (b) T. A. Skotheim, R. L. Elsenbaumer and J. R. Reynolds, *Handbook of Conducting Polymers*, 2nd ed., M. Dekker, New York, 1998; (c) J. Heinze, B. A. Frontana-Urbe and S. Ludwigs, *Chem. Rev.*, 2010, **110**, 4724.
 - (a) Y. Zhao, G. Chen, K. Mulla, I. Mahmud, S. Liang, P. Dongare, D. W. Thompson, L. N. Dawe and S. Bouzan, *Pure Appl. Chem.*, 2012, **84**, 1005; (b) M. Bendikov, F. Wudl and D. F. Perepichka, *Chem. Rev.*, 2004, **104**, 4891; (c) J. Roncali, *J. Mater. Chem.*, 1997, **7**, 2307.
 - (a) R. Carlier, P. Hapiot, D. Lorcy, A. Robert and A. Tallec, *Electrochim. Acta*, 2001, **46**, 3269; (b) N. Bellec, K. Boubekeur, R. Carlier, P. Hapiot, D. Lorcy and A. Tallec, *J. Phys. Chem. A*, 2000, **104**, 9750; (c) P. Hapiot, D. Lorcy, A. Tallec, R. Carlier and A. Robert, *J. Phys. Chem.*, 1996, **100**, 14823.
 - (a) D. Lorcy, M. Guerro, J.-F. Bergamini and P. Hapiot, *J. Phys. Chem. B*, 2013, **117**, 5188; (b) E. Gontier, N. Bellec, P. Brignou, A. Gohier, M. Guerro, T. Roisnel and D. Lorcy, *Org. Lett.*, 2010, **12**, 2386; (c) M. Guerro, R. Carlier, K. Boubekeur, D. Lorcy and P. Hapiot, *J. Am. Chem. Soc.*, 2003, **125**, 3159.
 - (a) K. Mulla, S. Liang, H. Shaik, E. A. Younes, A. Adronov and Y. Zhao, *Chem. Commun.*, 2015, **51**, 149; (b) S. Liang, Y. Zhao and A. Adronov, *J. Am. Chem. Soc.*, 2013, **136**, 970; (c) S. Liang, G. Chen and Y. Zhao, *J. Mater. Chem. C*, 2013, **1**, 5477; (d) S. Liang, G. Chen, J. Peddle and Y. Zhao, *Chem. Commun.*, 2012, **48**, 3100.
 - (a) G. Chen, I. Mahmud, L. N. Dawe, L. M. Daniels and Y. Zhao, *J. Org. Chem.*, 2011, **76**, 2701; (b) G. Chen, I. Mahmud, L. N. Dawe and Y. Zhao, *Org. Lett.*, 2010, **12**, 704.
 - G. Chen and Y. Zhao, *Org. Lett.*, 2014, **16**, 668.
 - (a) K. Mulla and Y. Zhao, *Tetrahedron Lett.*, 2014, **55**, 382; (b) K. Mulla, H. Shaik, D. W. Thompson and Y. Zhao, *Org. Lett.*, 2013, **15**, 4532; (c) K. Mulla, P. Dongare, D. W. Thompson and Y. Zhao, *Org. Biomol. Chem.*, 2012, **10**, 2542; (d) J. Massue, N. Bellec, M. Guerro, J.-F. Bergamini, P. Hapiot and D. Lorcy, *J. Org. Chem.*, 2007, **72**, 4655.
 - (a) T. M. Figueira-Duarte and K. Müllen, *Chem. Rev.*, 2011, **111**, 7260; (b) F. M. Winnik, *Chem. Rev.*, 1993, **93**, 587.
 - For recent examples, see: (a) N.-W. Wu, J. Zhang, D. Ciren, Q. Han, L.-J. Chen, L. Xu and H.-B. Yang, *Organometallics*, 2013, **32**, 2536; (b) K. Takemoto, M. Karasawa and M. Kimura, *ACS Appl. Mater. Interf.*, 2012, **4**, 6289; (c) P. D. Tran, A. Le Goff, J. Heidkamp, B. Jousset, N. Guillet, S. Palacin, H. Dau, M. Fontecave and V. Artero, *Angew. Chem. Int. Ed.*, 2011, **50**, 1371; (d) Y. Liu, Z.-L. Yu, Y.-M. Zhang, D.-S. Guo and Y.-P. Liu, *J. Am. Chem. Soc.*, 2008, **130**, 10431; (e) C. Ehli, G. M. A. Rahman, N. Jux, D. Balbinot, D. M. Guldi, F. Paolucci, M. Marcaccio, D. Paolucci, M. Melle-Franco, F. Zerbetto, S. Campidelli and M. Prato, *J. Am. Chem. Soc.*, 2006, **128**, 11222.
 - J. M. Casas-Solvas, J. D. Howgego and A. P. Davis, *Org. Biomol. Chem.*, 2014, **12**, 212.
 - G. Venkataramana, P. Dongare, L. N. Dawe, D. W. Thompson, Y. Zhao and G. J. Bodwell, *Org. Lett.*, 2011, **13**, 2240.
 - Spartan'10, Wavefunction Inc., Irvine, CA, USA.
 - (a) M. T. Stone, J. M. Heemstra and J. S. Moore, *Acc. Chem. Res.*, 2005, **39**, 11; (b) C. R. Ray and J. S. Moore, *Adv. Polym. Sci.*, 2005,

177, 91; (c) J. C. Nelson, J. G. Saven, J. S. Moore and P. G. Wolynes, *Science*, 1997, **277**, 1793.